New sensorless wavefront estimation approach for two photon scanning microscopy

J. Teixeira[#a], D. Champelovier[b,c], J-M. Conan[a], L. Mugnier[a], S. Meimon[a], N. Balla[b], S. Reichinnek[c], T. Tressard[c], R. Cossart[c], S. Monneret[b], H. Rigneault[b], and A. Malvache[b,c]

[a]ONERA – the French Aerospace Lab, F-92320 Châtillon, France
[b]Institut Fresnel, UMR 7249 CNRS, Aix-Marseille Université, F-13013 Marseille, France
[c]INMED, INSERM U901, Aix-Marseille Université, F-13273 Marseille, France

ABSTRACT

The landscape of biomedical research in neuroscience has changed dramatically in recent years as a result of spectacular progress in dynamic microscopy. In this context Adaptive Optics allows in-depth imaging by correcting aberrations induced by the biological sample, the key issue being then the ability to perform an accurate and reliable wavefront sensing (WFS). We present here a limitation of modal sensorless WFS in the case of a heterogeneous medium. We then build a new method called Axially-Locked Modal Sensorless (ALMS) that exploits these heterogeneities to overcome this limitation. The new method is simulated and compared to standard modal sensorless. The simulation results show a more accurate wavefront estimation even in the case of a strongly aberrated biological media.

Keywords: adaptive optics, microscopy, multi-photon, modal sensorless, axially-locked, sample dependence, neurobiology

1. INTRODUCTION

In vivo imaging of neuronal calcium dynamics using two-photon microscopy is an increasingly used method of choice to study neuronal activity at microcircuit level. In the dorsal region, CA1 of the hippocampus (the most optically accessible), this technique allows neuronal activity recording, in large fields of view containing hundreds of cells.[1] It has led to pioneering discovery of multineuron dynamics including, for example fear conditioning,[2] spatial navigation,[3–5] epilepsy[6] or quiet rest.[7] However, the implementation of this technique remains challenging as it requires, prior to cranial window implantation, surgery to remove the overlaying cortex, which introduces a high variability of "optical access" to the tissue. The main issues are the presence of blood from the capillaries and sometimes from small hemorrhage as well as the quality of the interface between the glass window and the brain surface. The former causes optical absorption and can be reduced by performing the surgery following water restriction to increase the viscosity of the blood,[1,5] while the latter causes optical aberrations. Furthermore, the densely packed layer of CA1 pyramidal neurons is located $200\mu m$ below the glass window covering the brain; the incoming laser beam is also perturbed by light scattering and optical aberrations during the propagation within the tissue. This problem should be tackled in order to improve detection of calcium probes which is impaired by the lowered contrast of the aberrated images. Even a modest improvement in contrast should lead to the detection of neural activity that otherwise is masked by background fluorescence from brain tissue.

Optical aberrations alter the quality of beam focusing, which in turn leads to reduced spatial resolution but also to lower signal and contrast. Thus, even when objects of interest are one order of magnitude larger than the diffraction limited laser focus (e.g. neurons soma are 10-15μm in diameter), the reduction of optical aberrations is critical to increasing the contrast of the fluorescence images. This improvement can be achieved using adaptive optics, a promising tool increasingly used for microscopy.[8–10] Adaptive optics is the process of quantifying optical aberrations through wavefront measurement and correcting them by the use of an adaptive correction element (deformable mirror DM or spatial light modulator SLM). Note that in point-scanning two-photon microscopy the correction is applied on the excitation beam alone and no correction is needed on the detection path. In

Further author information: Send correspondence to J.Teixeira: joel.teixeira@onera.fr

such microscopes, the wavefront can either be directly measured or indirectly estimated. Direct wavefront measurement relies on introducing a wavefront sensor such as a Shack-Hartmann in the detection part of the microscope. A point source in the sample is then imaged on the sensor. Direct methods have been proposed for two-photon imaging in weakly scattering samples where auto-fluorescence signals can be used to generate a highly localized signal,[11,12] but more complex methods such as coherence gating[13] or near-IR guide stars[14] are required to avoid out-of-focus fluorescence in highly scattering samples.

Indirect or sensorless wavefront estimation has the advantage of being easy-to-implement on existing systems as it relies on conventional imaging systems. This methods can be divided in two categories: intensity-based methods and image-based methods. In intensity-based methods, the optimization of the return flux is performed on a single fixed point (no scan is used).[15,16] Image-based methods, relies on successive image measurements with an engineered illuminating laser beam displaying different spatial shapes either in intensity (pupil segmentation[17]) or in phase (modal sensorless[18]). We study here image-based methods since for heterogeneous media, such as the mouse brain, images provide useful information for the wavefront estimation. Furthermore we concentrate on modal sensorless since the pupil segmentation method is considered too slow for *in vivo* imaging.[19]

In this paper we explore the applicability of the modal sensorless method to *in vivo* imaging of the hippocampus. We first demonstrate a limitation of the standard approach and we overcome this limitation with a new strategy called Axially-Locked Modal Sensorless (ALMS) that exploits the biological sample structure and automatically adjusts the focus depth. Gain brought by ALMS is quantified with numerical simulations.

In Sect. 2 we first recall the principle of modal sensorless wavefront sensing and we discuss a limitation of the method. We then present in Sect. 3 the new ALMS method. In Sect. 4 we compare ALMS with the standard modal sensorless through numerical simulations.

2. MODAL SENSORLESS AND SAMPLE DEPENDENCE

In the modal sensorless method,[18] one maps an image quality metric in phase space by applying successive wavefront deformations to the adaptive optics corrective element at a fixed depth. The "optimal" corrective wavefront shape is then assumed to be the one that maximizes the image quality metric. The usual metric is the mean image intensity (M1) and the usual basis for the phase space is the Zernike mode basis.

However, the "optimal" wavefront that maximizes the quality metric is not only linked to the wavefront deformation but also to the observed object. For instance, we have shown that, in two-photon microscopy, the mean image intensity M1 could be mathematically expressed as:[20]

$$\mathrm{M1} = \int \left[\iint \eta(x,y,z)\ dx\ dy \times \iint h_a^2(x,y,z)\ dx\ dy \right]\ dz = \int \bar{\eta}(z) \times \bar{H}_a(z)\ dz \tag{1}$$

where $\eta(x,y,z)$ and $\bar{\eta}(z)$ represent respectively the 3D object and its axial distribution, $h_a^2(x,y,z)$ and $\bar{H}_a(z)$ represent respectively the squared PSF and its axial axial distribution for given aberrations a. x and y represent the transverse coordinates and z the longitudinal one. This expression clearly shows that the mean image intensity M1 is not only related to the aberrations, but also to the object axial distribution.

As the amount of aberrations increases, the focal volume (i.e. the point spread function of the excitation beam) is distorted and enlarged, so that the maximum intensity in the focal volume decreases. It is therefore expected that the mean image intensity metric M1 is maximized when there are no aberration in the system. For instance, this is obvious in the case of a in-focus fluorescent bead. However, for certain spatial distributions of fluorophores, the modal sensorless method may lead to a biased wavefront estimation.

Figure 1 illustrate this problem. One can observe that, for a $10\mu m$-diameter fluorescent bead located $12\mu m$ out-of-focus, a metric maximum is obtained for 1.8 rad of coma aberration (Fig.1a). Indeed, when no aberrations are present the overlap between focal volume and the bead is minimal (Fig.1a and 1b). Increasing the amount of coma causes an elongation/distortion of the focal volume and increases the overlap with the out-of-focus bead (Fig.1c) and hence the metric M1.

In other words, for some fluorophore distributions, an increase of aberrations can increase the mean image intensity metric value while worsening the quality of the laser beam focus and thus degrading the overall resolution

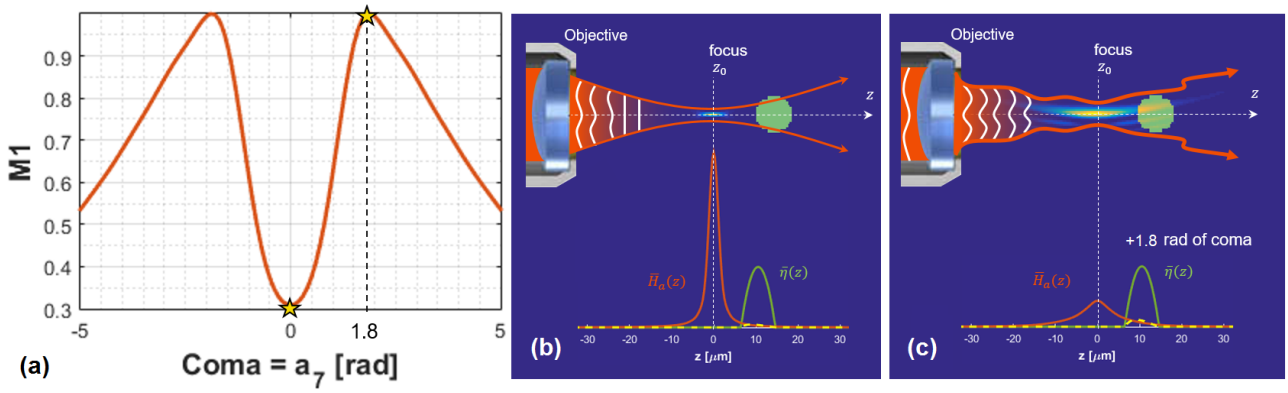

Figure 1: Sample-dependence in modal sensorless WFS: illustration on simulations for a $10\mu m$ diameter fluorescent bead out-of-focus. (a) Mean image intensity metric M1 as a function of coma ($a7$) amplitude. (b, c) Respective schematic illustration of the 2D axial profile xz (above) and axial distribution (under) of the point spread function and of the fluorescent bead for 0 and 1.8 rad of coma; the excitation beam propagates along the z axis.

and contrast of the data. In such undesirable situations, the wavefront estimation is thus biased and is said "sample dependent".

Note that this bias effect has been shown in third harmonic generation (THG) microscopy, where increasing the amount of aberrations could increase the THG mean intensity for some specific sample geometry.[21,22] This effect is also expected in two-photon excitation fluorescence microscopy.[16,22] It has been suggested to construct a specific basis said "displacement-free"[23,24] for the optimization but this does not prevent the elongation of the PSF induced for instance by coma aberration.

This example on an isolated object can be generalized to any heterogeneously labeled sample. The modal sensorless method may therefore lead to a biased estimation of the aberration that is linked to the volumetric distribution of contrast agent in the object.

To overcome the sample dependence issue we propose an improvement of the original modal optimization scheme described in the following section.

3. AXIALLY-LOCKED MODAL SENSORLESS

The inhomogeneous labeling of biological media thus results in the sample dependence issue with the current modal strategies. In contrast, we wish here to exploit our prior knowledge on the object 3D structure, in our case the presence of $10\mu m$ size neurons somas, in order to obtain a non-biased wavefront estimation. Instead of constraining the optimization to "stay away" from a strong fluorophore concentration such as neuron soma, we take the opposite strategy of "lock" on it, and optimize the aberrations around it. In this sense, we make use of the strongest light source in the vicinity, instead of fighting its influence on the optimization.

3.1 The optimization procedure

We thus designed a procedure called "Axially-Locked Modal Sensorless" (ALMS), which consists in performing the following steps (procedure illustrated on Fig. 2):

1. Find a local maximum of an intensity related metric in the axial (z) dimension
2. At this focusing depth, estimate the aberrations and apply the respective shape to the deformable mirror.
3. Repeat step 1. and step 2. to perform a fine tuning of both aberration estimation and focusing depth.

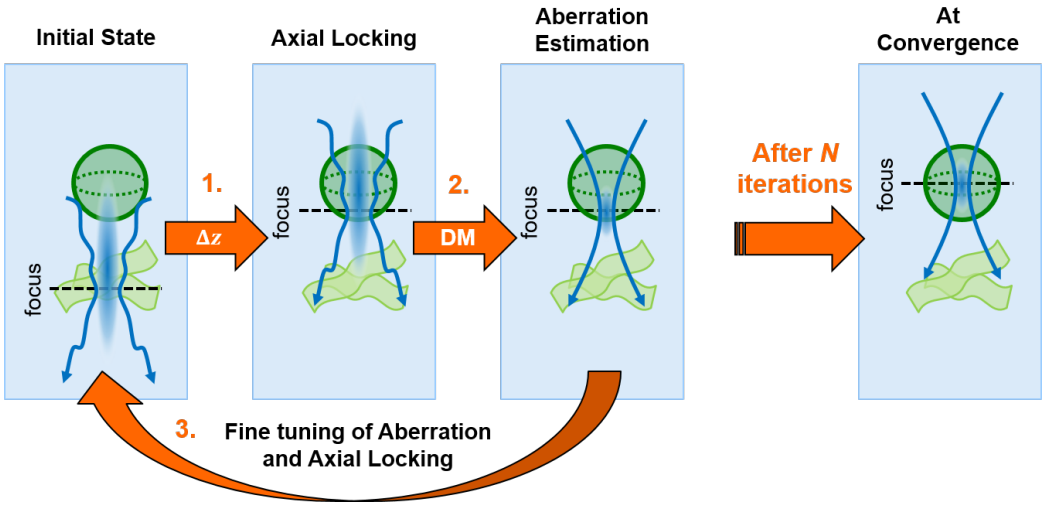

Figure 2: Illustration of the Axially-Locked Modal Sensorless (ALMS) method.

Contrary to previous works, ALMS strategy therefore allows controlled shifts in focusing depth - initially the procedure operates a coarse focus while fine tuning of defocus is performed iteratively. ALMS uses bright structures as guide stars naturally present in the sample to eliminate the risk of introducing aberrations during the optimization process.

Remains the choice of a relevant metric for the axial locking on the structures of interest.

3.2 The image quality metric

The axial locking step of the ALMS method requires a intensity-related metric that presents local maximum around the structures of interest. In the case of neuronal imaging, this structure is a labeled soma. To study the locking efficiency of various metrics, we used a 3D digitized sample representing a brain slab including one soma (centered at $2.88\mu m$) as well as dendrites, built using confocal images of GFP-expressing neurons in fixed hippocampus slices.

Figure 3 presents two transverse scans obtained at $2.88\mu m$ (plane where the soma is centered) and $8\mu m$ (plane essentially with dendrites). The mean image intensity M1 of each scan was calculated and we observe that M1 is higher for the scan with dendrites, *i.e.* it does not allow to lock on the soma. Actually Eq. 1 shows that the mean image intensity does not depend on the transverse (xy) structure of the object, it depends on its mean axial distribution and aberrations. So an image with few very bright pixels can obtain a lower mean value than an image with many faint pixels. We therefore need to investigate other intensity-related metrics.

We can observe that the image intensity variance (usually known as sharpness metric) M2 is higher for the the transverse scan where the soma is located. Indeed, it is known that the image variance is higher for images with few and very bright pixels which makes it better than M1 for the axial locking step.

However, one can still exploit more information from the obtained scans. Neurons somas are $\sim 10\mu m$ diameter compact structures. The presence of such structures can be enhanced by pre-filtering out low and high spatial frequencies of the image, to increase the contrast between soma and dendrites, before calculating the intensity variance. We call this metric "pre-filtered image variance" - M3.[20] The exact filtering parameters are defined such that the objects of interest (i.e. neurons soma) are highlighted. As displayed in Fig. 4, M3 improves the axial locking step by increasing the metric difference between the two scans. Thus, step 1 of our method consists in computing M3 values as a function of depth, and then setting the imaging plane at the depth that maximizes M3. We actually also use M3 in the other steps of ALMS.

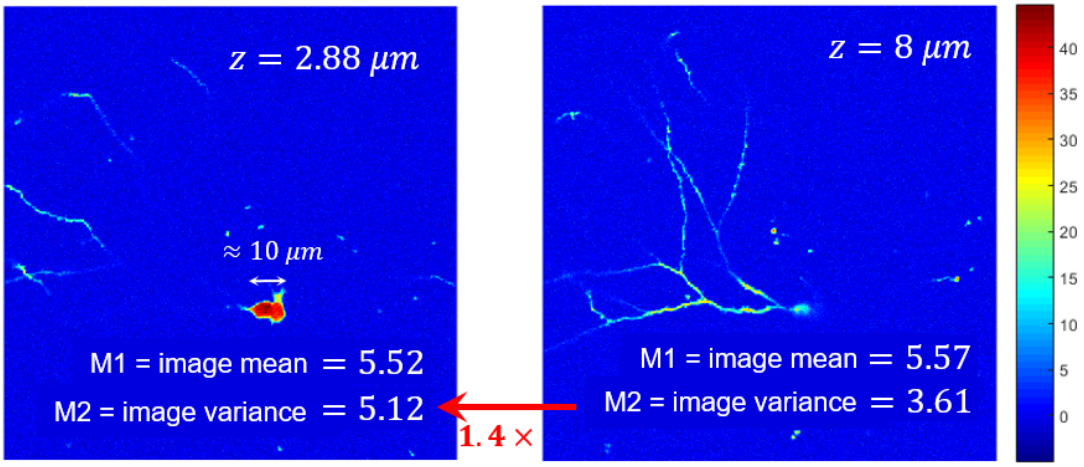

Figure 3: Images of two transverse scans at $2.88\mu m$ and $8\mu m$ on a 3D numerical model simulating a brain slab.

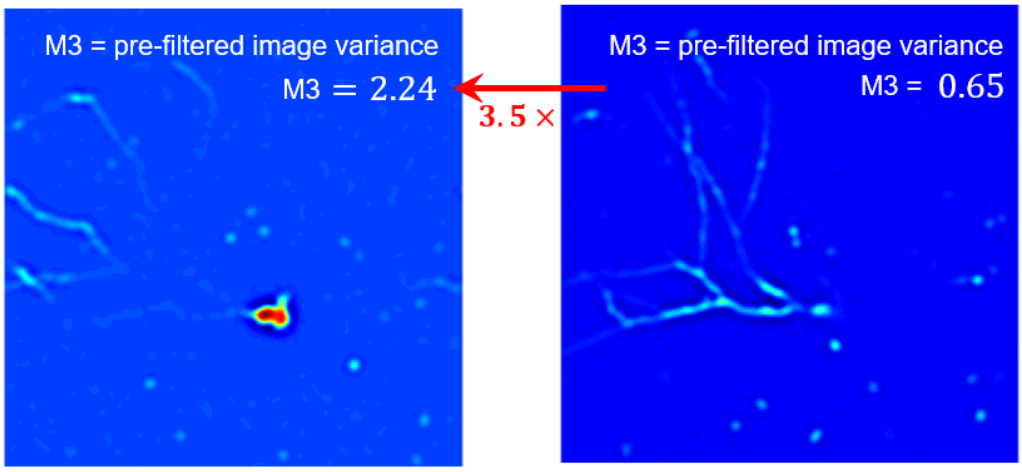

Figure 4: Filtered images of two transverse scans at $2.88\mu m$ and $8\mu m$ on a 3D numerical model simulating a brain slab. Low and high frequencies were pre-filtered to enhance $10\mu m$ diameter compact structures.

4. RESULTS

To quantify the improvement obtained with the ALMS method we compared, in simulation, an aberration estimation with the ALMS based on the pre-filtered image variance M3 and the standard modal sensorless based on the mean image intensity M1 (5 iterations for each method). We used the 3D model used for the metric study (Sec. 3.2) and we added a strongly aberrated wavefront ($\approx 8\text{rad}^2$) to simulate deep imaging in the hippocampus. Figure 5a shows the evolution of the focusing depth as function of iterations. By construction, the standard modal sensorless does not displace the initial focusing depth which is chosen by maximizing the respective metric before the procedure. In ALMS the focusing depth converges to the localization of the neuron soma center. Figure 5b shows the evolution of the residual wavefront variance as a function of iterations. One can observe that, at the last iteration, the standard modal sensorless leaves a residual wavefront with around 4.5 squared radians while ALMS provides a full wavefront correction.

This result shows that ALMS can perform a non-biased wavefront estimation even in strongly aberrated cases. ALMS is therefore a very promising strategy to perform deep *in vivo* imaging of heterogeneous labeled biological media.

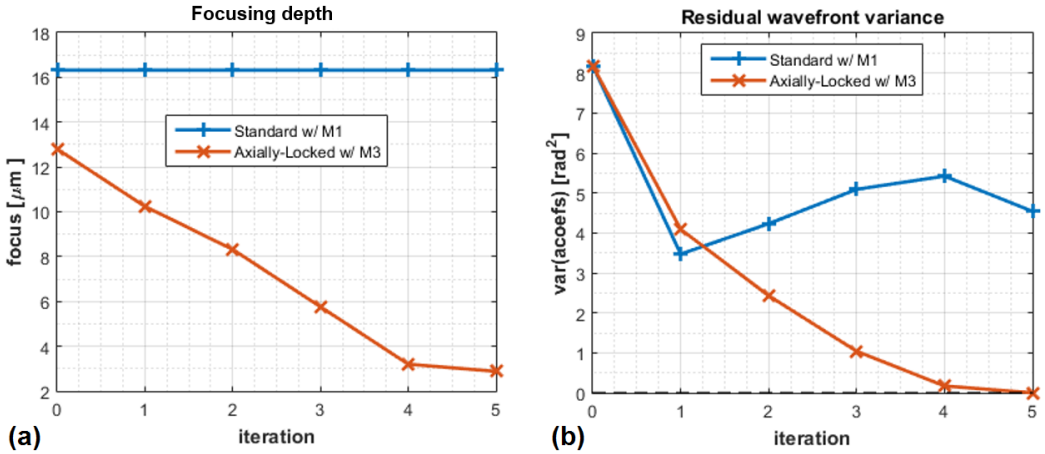

Figure 5: Performance comparison of the Axially-Locked Modal Sensorless (ALMS) and the standard modal sensorless methods; (a) Evolution of the focusing depth as a function of iteration. We recall that the neuron soma is located at around 2.88μm depth; (b) Evolution of the residual wavefront variance as a function of iteration.

5. CONCLUSION

We propose a new image-based adaptive optics method that is designed for imaging heterogeneously labeled scattering samples such as the pyramidal cell layer of the hippocampus. It relies on a specific metric which consists in filtering out very low and very high spatial frequencies of the image before calculating the intensity variance. Thanks to this "pre-filtered image variance metric", we exploit the stereotyped motif of the labeling (e.g. the neurons) to lock on the optimal layer depth before performing aberration estimation. Most importantly, we show that ALMS is very promising to enhance the image quality in deep *in vivo* imaging of the hippocampus as it performs a good correction of aberrations even in strongly aberrated scenarios.

Compared to direct measurement methods, our method is easy-to-implement as it only requires adding a wavefront correction device in a standard microscope. Furthermore, it can readily be applied on biologically relevant samples such as GCamP expressing neuron because it does not require isolated objects thanks to its low sensitivity to inhomogeneous labeling. We have as a matter of fact already obtained *ex vivo* and *in vivo* experimental results.[20] Additionally, this technique is suitable for all kinds of applications which involve fluorescence imaging in deep tissues.

ACKNOWLEDGMENTS

This work was supported by the INSERM, CNRS and ONERA. This project has received funding from the Agence Nationale de la Recherche (ANR11-INSB-0006, ANR-10-INSB-04-01, ANR-15-CE19-0018-01), the Aix-Marseille Université (ANR-11-IDEX-0001-02), the Fondation pour la Recherche Médicale (DBS20131128448), the European Research Council (ERC) under the European Union's FP7 and Horizon 2020 research and innovation program (grant agreement #242842 and #646925), from the DFG (Deutsche Forschungsgemeinschaft Project # RE 3657/1-1) and the WHRI Cofund (PCOFUND-GA-2013-608765).

REFERENCES

[1] Dombeck, D. A., Harvey, C. D., Tian, L., Looger, L. L., and Tank, D. W., "Functional imaging of hippocampal place cells at cellular resolution during virtual navigation," *Nature Neuroscience* **13**, 1433–1440 (Nov 2010).

[2] Lovett-Barron, M., Kaifosh, P., Kheirbek, M. A., Danielson, N., Zaremba, J. D., Reardon, T. R., Turi, G. F., Hen, R., Zemelman, B. V., and Losonczy, A., "Dendritic inhibition in the hippocampus supports fear learning," *Science* **343**(6173), 857–863 (2014).

[3] Sheffield, M. E. J. and Dombeck, D. A., "Calcium transient prevalence across the dendritic arbour predicts place field properties," *Nature* **517**, 200–204 (Jan 2015). Letter.

[4] Danielson, N. B., Zaremba, J. D., Kaifosh, P., Bowler, J., Ladow, M., and Losonczy, A., "Sublayer-specific coding dynamics during spatial navigation and learning in hippocampal area ca1," *Neuron* **91**(3), 652–665 (2016).

[5] Villette, V., Malvache, A., Tressard, T., Dupuy, N., and Cossart, R., "Internally recurring hippocampal sequences as a population template of spatiotemporal information," *Neuron* **88**(2), 357–366 (2015).

[6] Feldt Muldoon, S., Soltesz, I., and Cossart, R., "Spatially clustered neuronal assemblies comprise the microstructure of synchrony in chronically epileptic networks," *Proceedings of the National Academy of Sciences* **110**(9), 3567–3572 (2013).

[7] Malvache, A., Reichinnek, S., Villette, V., Haimerl, C., and Cossart, R., "Awake hippocampal reactivations project onto orthogonal neuronal assemblies," *Science* **353**(6305), 1280–1283 (2016).

[8] Booth, M. J., "Adaptive optical microscopy: the ongoing quest for a perfect image," *Light: Science & Applications* **3**(4), e165 (2014).

[9] Kubby, J. A., [*Adaptive Optics for Biological Imaging*], CRC press (2013).

[10] Booth, M., Andrade, D., Burke, D., Patton, B., and Zurauskas, M., "Aberrations and adaptive optics in super-resolution microscopy," *Microscopy* **64**(4), 251 (2015).

[11] Aviles-Espinosa, R., Andilla, J., Porcar-Guezenec, R., Olarte, O. E., Nieto, M., Levecq, X., Artigas, D., and Loza-Alvarez, P., "Measurement and correction of in vivo sample aberrations employing a nonlinear guide-star in two-photon excited fluorescence microscopy," *Biomed. Opt. Express* **2**, 3135–3149 (Nov 2011).

[12] Wang, J., Léger, J.-F., Binding, J., Boccara, A. C., Gigan, S., and Bourdieu, L., "Measuring aberrations in the rat brain by coherence-gated wavefront sensing using a linnik interferometer," *Biomed. Opt. Express* **3**, 2510–2525 (Oct 2012).

[13] Tao, X., Norton, A., Kissel, M., Azucena, O., and Kubby, J., "Adaptive optical two-photon microscopy using autofluorescent guide stars," *Opt. Lett.* **38**, 5075–5078 (Dec 2013).

[14] Wang, K., Sun, W., Richie, C. T., Harvey, B. K., Betzig, E., and Ji, N., "Direct wavefront sensing for high-resolution in vivo imaging in scattering tissue," *Nature Communications* **6**, 7276 EP – (Jun 2015). Article.

[15] Tang, J., Germain, R. N., and Cui, M., "Superpenetration optical microscopy by iterative multiphoton adaptive compensation technique," *Proceedings of the National Academy of Sciences* **109**, 8434–8439 (May 2012). 22586078[pmid].

[16] Galwaduge, P. T., Kim, S. H., Grosberg, L. E., and Hillman, E. M. C., "Simple wavefront correction framework for two-photon microscopy of in-vivo brain," *Biomed. Opt. Express* **6**, 2997–3013 (Aug 2015).

[17] Ji, N., Milkie, D. E., and Betzig, E., "Adaptive optics via pupil segmentation for high-resolution imaging in biological tissues," *Nature Methods* **7**, 141–147 (Feb 2010).

[18] Débarre, D., Botcherby, E. J., Watanabe, T., Srinivas, S., Booth, M. J., and Wilson, T., "Image-based adaptive optics for two-photon microscopy," *Opt. Lett.* **34**, 2495–2497 (Aug 2009).

[19] Wang, C., Liu, R., Milkie, D. E., Sun, W., Tan, Z., Kerlin, A., Chen, T.-W., Kim, D. S., and Ji, N., "Multiplexed aberration measurement for deep tissue imaging in vivo," *Nature Methods* **11**, 1037–1040 (Oct 2014). Brief Communication.

[20] Champelovier, D., Teixeira, J., Conan, J.-M., Balla, N., Mugnier, L., Tressard, T., Reichinnek, S., Meimon, S., Cossart, R., Rigneault, H., Monneret, S., and Malvache, A., "Image-based adaptive optics for in vivo imaging in the hippocampus," *Nature Scientific Reports* (2017 in press).

[21] Olivier, N., Débarre, D., and Beaurepaire, E., "Dynamic aberration correction for multiharmonic microscopy," *Opt. Lett.* **34**, 3145–3147 (Oct 2009).

[22] Thayil, A., Jesacher, A., Wilson, T., and Booth, M. J., "The influence of aberrations in third harmonic generation microscopy," *Journal of Optics* **12**(8), 084009 (2010).

[23] Thayil, A. and Booth, M., "Self calibration of sensorless adaptive optical microscopes," *Journal of the European Optical Society - Rapid publications* **6**(0) (2011).

[24] Facomprez, A., Beaurepaire, E., and Débarre, D., "Accuracy of correction in modal sensorless adaptive optics," *Opt. Express* **20**, 2598–2612 (Jan 2012).